A NON-DIMENSIONAL STUDY ON BOTH ANALYTIC AND NUMERIC THERMO-ELASTIC BEHAVIOR OF FUNCTIONALLY GRADED THICK-WALLED CYLINDERS UNDER A COMBINATION OF THERMO-MECHANICAL LOADS

H. Asgharzadeh Shirazi[1], M. Abedi[2], A. Asnafi [3]*, M. Salimi[1]
[1]School of Mechanical Engineering, Iran University of Science and Technology, Narmak, 16846-13114, Tehran
[2]School of Mechanical Engineering, Shiraz University, Shiraz 71348-13668, Iran
[3]Hydro-Aeronautical Research Center, Shiraz University, Shiraz, 71348-13668, Iran.

ABSTRACT

Efforts Using non-dimensional parameters, the governing equations of homogeneous and heterogeneous cylinders made of functionally graded material (FGM) were derived under a combination of thermo-mechanical loads. The equations were solved analytically and numerically in a severe temperature and pressure gradient environment. The radial and circumferential stresses together with the radial displacement of FGM cylinder were analytically evaluated and then compared to conventional homogeneous ones. Besides, in order to assess the accuracy of derived equations, a numerical solution (NS) was performed using finite element method. It was shown that the numerical solution was in accordance to the analytical solution (AS). The results of present work show that the use of FGM can optimize the thermo-elastic performance of the cylinders which are exposed to the joint mechanical and thermal loads.

KEYWORDS: *Thick-walled cylinder; FGM heterogeneous materials; Finite element method;*

1.0 INTRODUCTION

Metals and many composites with high levels of strength to weight ratio, have been successfully employed in the fields of mechanical engineering; however, they do not demonstrate good performance in the environments with high temperature conditions. On the other hand, materials such as ceramics show excellent performance in high-temperature environments while, they are sometimes unreliable in terms of strength and stiffness. In order to encompass these conversely goals in some applications, the functionally graded materials (FGMs) have been introduced. First time, they were proposed in the mid-1980s in Japan as a thermal coating for some engineering applications (Mahamood, Akinlabi, Shukla & Pityana, 2012). Japanese researchers used this developed composite as a thermal barrier across a 10 mm thickness with two different temperatures of 1000 and 2000K on both sides of the area (Mahamood et al., 2012). Generally, FGMs are heterogeneous composites whose properties such as modulus of elasticity, thermal conductivity and mass density, change gradually from one side to the other side of the material domain. These materials are well-known for

* Corresponding author email: asnafi@shirazu.ac.ir

their ability in isolating or separating two different environments with diverged designed goals. These materials can support high temperatures and extreme temperature gradients as they do for mechanical loads. As practical examples, the internal parts of combustion engines, turbines and power plants are under high temperature and severe temperature gradient jointly. It is worth noting that the low thermal conductivity and low coefficient of thermal expansion of FGM materials allow them to accept high temperatures and severe temperature gradients (Azadi, 2009; Azadi & Shariyat, 2010; Damircheli & Azadi, 2011).

In recent years, many works have been conducted on the behavior of functionally graded materials (Tuntucu & Ozturk, 2001). In 2001, Tutuncu and Ozturk (2001) used the infinitesimal theory of elasticity to obtain closed-form solutions for both stress and displacement in functionally graded cylindrical and spherical vessels subjected to internal pressure. In 2008, Argeso and Eraslan (2008) assessed an estimation of the thermo-elastic response of cylinders and tubes, using temperature-dependent physical properties. Using exact closed-form solutions based on plane elasticity theory, Nejad, Abedi, Lotfian and Ghannad (2012) studied both the stress and displacement profiles in a thick spherical shell made of functionally graded materials with exponential-varying elasticity modulus under uniform pressure. They assumed plane strain condition and considered a fixed value for the Poisson's ratio (Nejat et al.,2012). In 2012, Bayat, Ghannad and Torabi (2012) studied a functionally graded thick-walled hollow sphere on the assumption of one-dimensional steady temperature distribution. They supposed the thermal and mechanical properties of sphere to be varied exponentially in the radial direction (Bayat et al., 2012).

Using non-dimensional parameters, this research attempts to develop thermo-elastic analysis of thick-walled structures like cylinder and disk made of functionally graded materials. Therefore, the aim of this paper is to improve the thick-walled cylinder behaviors by proposing dimensionless governing equations of homogeneous and heterogeneous FGM cylinder under thermo-mechanical loads. The results were also compared to other works and discussed.

2.0 FUNDAMENTAL EQUATIONS

In the plane elasticity theory, it is assumed that the cross-section plane which is perpendicular to the central axis of the cylinder will remain planar and perpendicular to the central axis after applying pressure and deformation. Furthermore, it is supposed that the radial deformations along the perimeter remain fixed but vary in radial direction. Theoritically, radial deformations dependent only on the radius $u_r(r)$. In order to solve the problem, a hollow cylinder of non-homogeneous FGM material with inner and outer radii of r_i and r_o under uniform internal and external pressures of P_i and P_o and the internal and external temperature surfaces of T_i and T_o, is considered. Figure 1 shows a section of the assumed cylinder under combined mechanical and thermal loading.

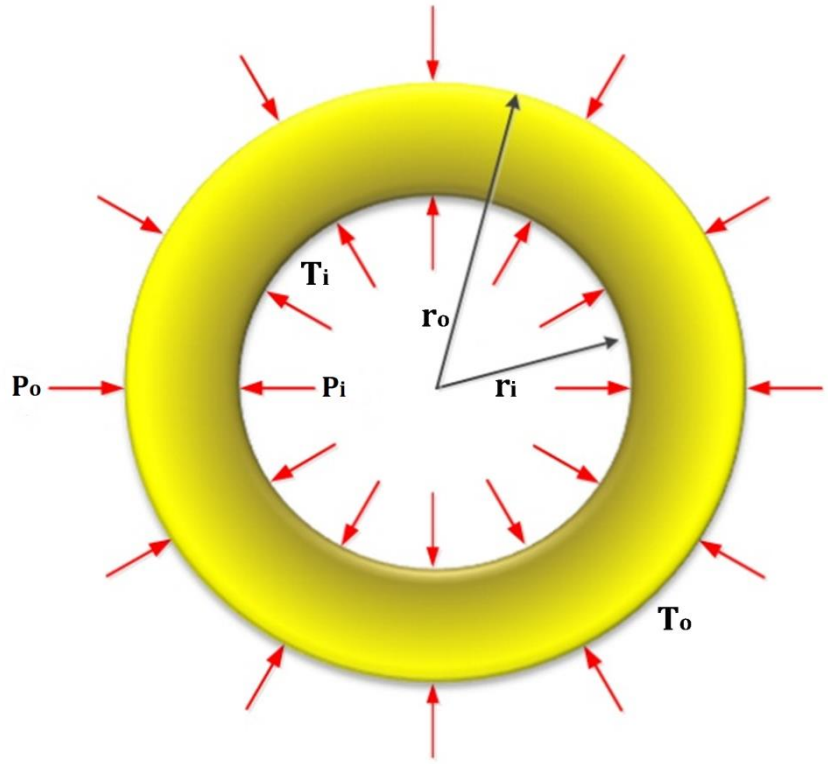

(a)

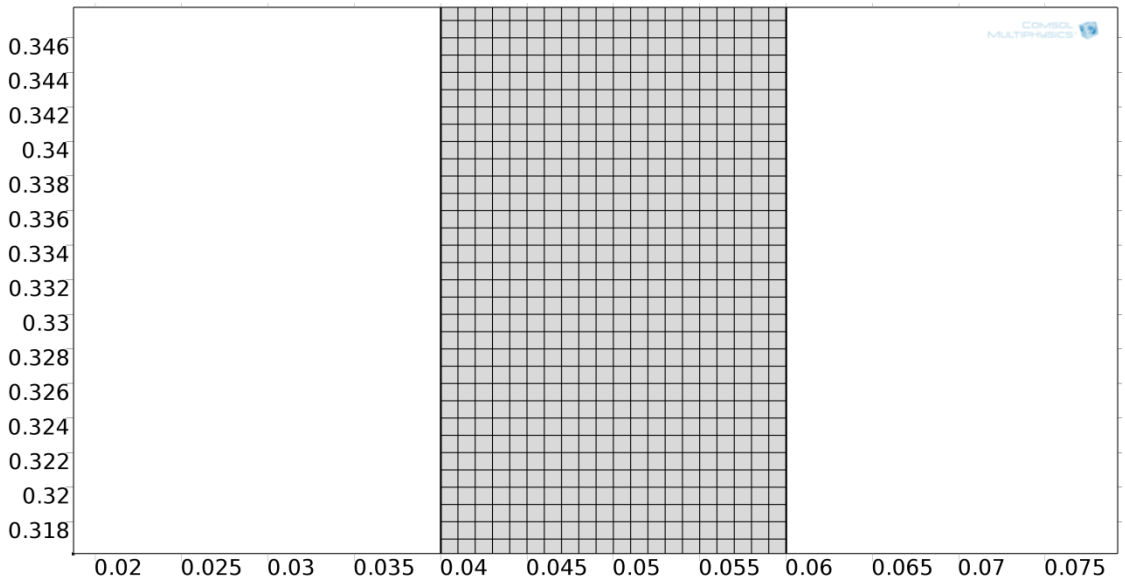

(b)

Figure 1. (a) Cross-section of a thick-walled cylinder with internal radius "r_i" and external radius "r_o", (b) Finite element mesh region.

Due to axisymmetric condition, material properties, loads and boundary conditions and according to plane elastic theory, the shear stresses and strains become all zero. Thus, the normal strains are:

$$\varepsilon_r = \frac{1}{E}\left(\sigma_r - \upsilon\sigma_\theta - \upsilon\sigma_z\right) + \alpha T \tag{1}$$

$$\varepsilon_\theta = \frac{1}{E}\left(\sigma_\theta - \upsilon\sigma_r - \upsilon\sigma_z\right) + \alpha T \tag{2}$$

$$\varepsilon_z = \frac{1}{E}\left(\sigma_z - \upsilon\sigma_r - \upsilon\sigma_\theta\right) + \alpha T \tag{3}$$

where E is the elasticity modulus, υ is Poisson's ratio, α is coefficient of thermal expansion and T is the temperature gradient. Moreover, σ_r, σ_θ and σ_z indicate normal stresses and ε_r, ε_θ and ε_z denote normal strains in r, θ and z directions, respectively. For plane strain condition in cylinders, normal strain in z direction turns into zero i.e. $\varepsilon_z=0$; so Eq. (3) develops into:

$$\sigma_z = \upsilon\left(\sigma_r + \sigma_\theta\right) - E\alpha T \tag{4}$$

By substituting Eq. (4) into Eqs. (1) and (2), we have:

$$\varepsilon_r = \frac{1}{E}\left[\left(1-\upsilon\right)\left(1+\upsilon\right)\sigma_r - \upsilon\left(1+\upsilon\right)\sigma_\theta\right] + \left(1+\upsilon\right)\alpha T \tag{5}$$

$$\varepsilon_\theta = \frac{1}{E}\left[\left(1-\upsilon\right)\left(1+\upsilon\right)\sigma_\theta - \upsilon\left(1+\upsilon\right)\sigma_r\right] + \left(1+\upsilon\right)\alpha T \tag{6}$$

Rewriting Eqs. (5) and (6) for stresses results in:

$$\sigma_r = \frac{E}{\left(1-2\upsilon\right)\left(1+\upsilon\right)}\left[\left(1-\upsilon\right)\varepsilon_r + \upsilon\varepsilon_\theta - \left(1+\upsilon\right)\alpha T\right] \tag{7}$$

$$\sigma_\theta = \frac{E}{\left(1-2\upsilon\right)\left(1+\upsilon\right)}\left[\upsilon\varepsilon_r + \left(1-\upsilon\right)\varepsilon_\theta - \left(1+\upsilon\right)\alpha T\right] \tag{8}$$

Now, Eqs. (7) and (8) can be rearranged to the following general form:

$$\begin{pmatrix}\sigma_r\\ \sigma_\theta\end{pmatrix} = E\begin{pmatrix}A_1 & A_2 & A_1+2A_2\\ A_2 & A_1 & A_1+2A_2\end{pmatrix}\begin{pmatrix}\varepsilon_r\\ \varepsilon_\theta\\ -\alpha T\end{pmatrix} \tag{9}$$

in which A_1 *and* A_2 relate to the Poisson's ratio as:

$$\begin{cases} A_1 = \dfrac{1-\upsilon}{\left(1-2\upsilon\right)\left(1+\upsilon\right)} \\ A_2 = \dfrac{\upsilon}{\left(1-2\upsilon\right)\left(1+\upsilon\right)} \end{cases} \tag{10}$$

In axisymmetric condition, all displacements become zero except for radial displacement (u_r). The radial displacement, of course, is a function of polar radius r only; therefore, strain-displacement relations in axisymmetric condition in cylindrical coordinate will be:

$$\begin{cases} \varepsilon_r = \dfrac{du_r}{dr} = \dfrac{P_i}{E_i}\dfrac{dU}{dR} \\ \varepsilon_\theta = \dfrac{u_r}{r} = \dfrac{P_i}{E_i}\dfrac{U}{R} \end{cases} \tag{11}$$

where E_i is the elasticity modulus of internal surface. Now, the dimensionless radius R and the dimensionless radial displacement U can be defined as:

$$R = \frac{r}{r_i} \tag{12}$$

$$U = \frac{E_i u_r}{r_i P_i} \tag{13}$$

Substituting Eq. (11) into Eq. (9) yields:

$$\begin{pmatrix} \bar{\sigma}_r \\ \bar{\sigma}_\theta \end{pmatrix} = \bar{E} \begin{pmatrix} A_1 & A_2 & A_1 + 2A_2 \\ A_2 & A_1 & A_1 + 2A_2 \end{pmatrix} \begin{pmatrix} \dfrac{dU}{dR} \\ \dfrac{U}{R} \\ -\Theta \bar{\alpha} \bar{T} \end{pmatrix} \tag{14}$$

where:

$$\bar{\sigma} = \frac{\sigma}{P_i}, \quad \bar{E} = \frac{E}{E_i}, \quad \bar{\alpha} = \frac{\alpha}{\alpha_i}, \quad \bar{T} = \frac{T}{T_i}, \quad \Theta = \frac{\left(A_1 + 2A_2\right) E_i \alpha_i T_i}{A_1 P_i} \tag{15}$$

In Eq. (15), α_i is the thermal expansion coefficient of cylinder internal surface. Neglecting the body forces, the equilibrium equation in axisymmetric conditions and in cylindrical coordinates will be:

$$\frac{d\sigma_r}{dr} + \frac{\sigma_r - \sigma_\theta}{r} = 0 \tag{16}$$

It can also be expressed as:

$$\frac{d\bar{\sigma}_r}{dR} + \frac{\bar{\sigma}_r - \bar{\sigma}_\theta}{R} = 0 \; ; \quad \begin{cases} \bar{\sigma}_r = \dfrac{\sigma_r}{P_i} \\ \bar{\sigma}_\theta = \dfrac{\sigma_\theta}{P_i} \end{cases} \tag{17}$$

Replacing Eq. (14) in Eq. (17) gives up:

$$\frac{d^2U}{dR^2}+\frac{1}{R}\left(1+\frac{Rd\bar{E}}{\bar{E}dR}\right)\frac{dU}{dR}-\frac{1}{R^2}\left(1-\frac{A_2}{A_1}\frac{Rd\bar{E}}{\bar{E}dR}\right)U=F\left(R\right) \tag{18}$$

where

$$F\left(R\right)=\frac{\Theta}{\bar{E}}\frac{d\left(\bar{E}\bar{\alpha}\bar{T}\right)}{dR} \tag{19}$$

Eq. (18) is a Bessel-like second order differential equation with general solution as in (Kreyszig, 2010):

$$U\left(R\right)=C_1G\left(R\right)+C_2H\left(R\right)+I\left(R\right) \tag{20}$$

where C_1 and C_2 are coefficients that can be calculated easily from the boundary conditions. $H(R)$ and $G(R)$ are general solutions; while $I(R)$ is the particular solution of the differential equation. The particular solution of the differential equation can be calculated as (Kreyszig, 2010):

$$I\left(R\right)=-G\left(R\right)\int\frac{F\left(R\right)H\left(R\right)}{W\left(R\right)}dR+H\left(R\right)\int\frac{F\left(R\right)G\left(R\right)}{W\left(R\right)}dR \tag{21}$$

where:

$$W\left(R\right)=G\left(R\right)\frac{dH\left(R\right)}{dR}-H\left(R\right)\frac{dG\left(R\right)}{dR} \tag{22}$$

To solve Eq. (18), a particular relation must be firstly attributed to the mechanical properties. Power function is the most common function for cylindrical hollow tubes. For constant Poisson's ratio (v), the elasticity modulus (E), the thermal expansion coefficient (α) and thermal conductivity (k) can be considered as:

$$E\left(R\right)=E_iR^{n_1} \tag{23}$$

$$\alpha\left(R\right)=\alpha_iR^{n_2} \tag{24}$$

$$k\left(R\right)=k_iR^{n_3} \tag{25}$$

where k_i is the thermal conductivity on the inner surface of the cylinder and n_1, n_2 and n_3 are material parameters. The homogeneous part of the Eq. (18) can be also obtained just by applying Eqs. (23) to (25):

$$R^2\frac{d^2U}{dR^2}+\left(n_1+1\right)R\frac{dU}{dR}-\left(1-\frac{A_2}{A_1}n_1\right)U=0 \tag{26}$$

Eq. (26) demonstrates an Euler-Cauchy equation. Assuming $U=R^m$, the characteristic equation can be achieved as:

$$m^2+n_1m-\left(1-\frac{A_2}{A_1}n_1\right)=0 \tag{27}$$

The roots of Eq. (27) are:

$$m_{1,2} = \frac{-n_1 \pm \sqrt{\Delta}}{2} \quad ; \Delta = n_1^2 - \frac{4A_2}{A_1} n_1 + 4 \tag{28}$$

Given the limitations of Poisson's ratio ($0<\upsilon<0.5$), the value of Δ is always positive. As a result, m_1 and m_2 always have distinct real values. Thus, the general solutions of $G(R)$ and $H(R)$ are:

$$\begin{cases} G(R) = R^{m_1} \\ H(R) = R^{m_2} \end{cases} \tag{29}$$

Substituting Eq. (29) into Eq. (22) results in:

$$W(R) = (m_2 - m_1) R^{m_1 + m_2 - 1} \tag{30}$$

Additionally, by substituting Eqs. (29) and (30) in Eq. (21), one can reach such the following relation:

$$I(R) = \frac{1}{m_2 - m_1} \left[-R^{m_1} \int R^{-m_1+1} F(R) dR + R^{m_2} \int R^{-m_2+1} F(R) dR \right] \tag{31}$$

In order to calculate the particular solution stated in the above equation, the term $F(R)$ should be expressed explicitly; However, in order to calculate $F(R)$, the relation of temperature gradient T should be obtained in explicit form and in terms of polar radius r.

2.1 Axisymmetric Heat Transfer Equation

The steady state heat transfer in cylindrical coordinate under axisymmetric condition can be obtained using the following famous ODE (Rohsenow & Warren,1998):

$$\frac{d}{dr}\left(kr \frac{dT}{dr} \right) = 0 \tag{32}$$

With reference to Eq. (25), the above equation can be expressed as:

$$\frac{d}{dR}\left(R^{n_3+1} \frac{d\bar{T}}{dR} \right) = 0 \tag{33}$$

Relative to the value of n_i, two cases of $n_i=0$ and $n_i\neq0$ must be studied and analyzed.

2.1.1 Case 1 $n_i\neq0$

In this case, the solution of the differential equation becomes:

$$\bar{T} = D_1 R^{-n_3} + D_2 \tag{34}$$

where D_1 and D_2 are constants that can be calculated from the following boundary conditions:

$$\begin{cases} T\left(r=r_i\right)=T_i \\ T\left(r=r_o\right)=T_o \end{cases} \Rightarrow \begin{cases} \bar{T}\left(R=1\right)=1 \\ \bar{T}\left(R=K\right)=T^* \end{cases} \tag{35}$$

Note also that:

$$\begin{cases} K=\dfrac{r_o}{r_i} \\ T^*=\dfrac{T_o}{T_i} \end{cases} \tag{36}$$

By applying the boundary conditions, one can attain such the following relations:

$$\begin{cases} D_1=\dfrac{1-T^*}{1-K^{-n_3}} \\ D_2=\dfrac{T^*-K^{-n_3}}{1-K^{-n_3}} \end{cases} \tag{37}$$

Thus, in this case, $F(R)$ in Eq. (18) can be obtained by substituting Eqs. (23), (24) and (37) into Eq. (19):

$$F\left(R\right)=\left(n_1+n_2-n_3\right)D_1\Theta R^{n_2-n_3-1}+\left(n_1+n_2\right)D_2\Theta R^{n_2-1} \tag{38}$$

Consequently, the particular solution $I(R)$, will be accomplished by substituting Eq. (37) into Eq. (31) as:

$$I\left(R\right)=C_3R^{n_2-n_3+1}+C_4R^{n_2+1} \tag{39}$$

where:

$$\begin{cases} C_3=\dfrac{\left(n_1+n_2-n_3\right)D_1\Theta}{\left(-m_1+n_2-n_3+1\right)\left(-m_2+n_2-n_3+1\right)} \\ C_4=\dfrac{\left(n_1+n_2\right)D_2\Theta}{\left(-m_1+n_2+1\right)\left(-m_2+n_2+1\right)} \end{cases} \tag{40}$$

Now, the complete solution for $U(R)$ is the sum of homogenous and particular solutions, i.e.

$$U\left(R\right)=C_1R^{m_1}+C_2R^{m_2}+C_3R^{n_2-n_3+1}+C_4R^{n_2+1} \tag{41}$$

Finally, by substituting Eqs. (23), (24), (34) and (40) into Eq. (14), the resulting radial and circumferential stress expressions are:

$$\bar{\sigma}_r=Q_{11}R^{m_1+n_1-1}+Q_{12}R^{m_2+n_1-1}+Q_{13}R^{n_1+n_2-n_3}+Q_{14}R^{n_1+n_2} \tag{42}$$

$$\bar{\sigma}_\theta=Q_{21}R^{m_1+n_1-1}+Q_{22}R^{m_2+n_1-1}+Q_{23}R^{n_1+n_2-n_3}+Q_{24}R^{n_1+n_2} \tag{43}$$

where:

$$\begin{aligned} Q_{11} &= \left(m_1 A_1 + A_2\right) C_1 & Q_{21} &= \left(A_1 + m_1 A_2\right) C_1 \\ Q_{12} &= \left(m_2 A_1 + A_2\right) C_2 & Q_{22} &= \left(A_1 + m_2 A_2\right) C_2 \\ Q_{13} &= \left(n_2 - n_3 + 1\right) A_1 C_3 + A_2 C_3 - A_1 D_1 \Theta & Q_{23} &= \left(n_2 - n_3 + 1\right) A_2 C_3 + A_1 C_3 - A_1 D_1 \Theta \\ Q_{14} &= \left(n_2 + 1\right) A_1 C_4 + A_2 C_4 - A_1 D_2 \Theta & Q_{24} &= \left(n_2 + 1\right) A_2 C_4 + A_1 C_4 - A_1 D_2 \Theta \end{aligned} \tag{44}$$

In Eqs. (41), (42) and (43) the constants C_1 and C_2 are still unknown. As mentioned previously, these constants must be calculated from mechanical boundary conditions i.e.

$$\begin{cases} \sigma_r\left(r = r_i\right) = -P_i \\ \sigma_r\left(r = r_o\right) = -P_o \end{cases} \Rightarrow \begin{cases} \bar{\sigma}_r\left(R = 1\right) = -1 \\ \bar{\sigma}_r\left(R = K\right) = -P^* \end{cases} \tag{45}$$

in which:

$$P^* = \frac{P_o}{P_i} \tag{46}$$

By applying the boundary conditions of Eq. (45), constants C_1 and C_2 are obtained as:

$$C_1 = \left(\frac{K^{m_2+n_1-1} - K^{n_1+n_3-n_4}}{K^{m_1+n_1-1} - K^{m_2+n_1-1}} Q_{13} + \frac{K^{m_2+n_1-1} - K^{n_1+n_3}}{K^{m_1+n_1-1} - K^{m_2+n_1-1}} Q_{14} + \frac{K^{m_2+n_1-1} - P^*}{K^{m_1+n_1-1} - K^{m_2+n_1-1}} \right) \Big/ \left(m_1 A_1 + A_2\right) \tag{47}$$

$$C_2 = \left(\frac{K^{m_1+n_1-1} - K^{n_1+n_3-n_4}}{K^{m_2+n_1-1} - K^{m_1+n_1-1}} Q_{13} + \frac{K^{m_1+n_1-1} - K^{n_1+n_3}}{K^{m_2+n_1-1} - K^{m_1+n_1-1}} Q_{14} + \frac{K^{m_1+n_1-1} - P^*}{K^{m_2+n_1-1} - K^{m_1+n_1-1}} \right) \Big/ \left(m_2 A_1 + A_2\right) \tag{48}$$

It is obvious that the calculation of the constants C_1 and C_2, will subsequently results in the non-dimensional radial displacement U together with the non-dimensional radial and circumferential stresses σ_r and σ_θ.

2.1.2 Case 2 $n_i = 0$

With the same procedure, the solution of the differential equation becomes:

$$\bar{T} = D_1 \ln\left(R\right) + D_2 \tag{49}$$

where D_1 and D_2 are the constants that must be calculated from the thermal boundary conditions expressed in Eq. (35):

$$\begin{cases} D_1 = \dfrac{T^* - 1}{\ln\left(K\right)} \\ D_2 = 1 \end{cases} \tag{50}$$

Thus, in this case by substituting Eqs. (23), (24) and (50) into Eq. (19), $F(R)$ turns into:

$$F\left(R\right) = \left(n_1 + n_2\right) D_1 \Theta R^{n_2 - 1} \ln\left(R\right) + \left[D_1 + \left(n_1 + n_2\right) D_2\right] \Theta R^{n_2 - 1} \tag{51}$$

Consequently, the particular solution $I(R)$ will be realized by substituting Eq. (51) in Eq. (31):

$$I\left(R\right)=C_3R^{n_2+1}\ln\left(R\right)+C_4R^{n_2+1} \tag{52}$$

where:

$$\begin{cases} C_3=\dfrac{\left(n_1+n_2\right)D_1\Theta}{\left(-m_1+n_2+1\right)\left(-m_2+n_2+1\right)} \\ C_4=\dfrac{D_1\Theta+\left(n_1+n_2\right)D_2\Theta}{\left(-m_1+n_2+1\right)\left(-m_2+n_2+1\right)}-\dfrac{\left(n_1+2n_2+2\right)\left(n_1+n_2\right)D_1\Theta}{\left(-m_1+n_2+1\right)^2\left(-m_2+n_2+1\right)^2} \end{cases} \tag{53}$$

The complete solution for $U(R)$, which is the sum of homogenous and particular solutions, develops into:

$$U\left(R\right)=C_1R^{m_1}+C_2R^{m_2}+C_3R^{n_2+1}\ln\left(R\right)+C_4R^{n_2+1} \tag{54}$$

At last, by substituting Eqs. (23), (24), (49) and (54) into Eq. (14), the resulting radial and circumferential stress expressions are:

$$\bar{\sigma}_r=Q_{11}R^{m_1+n_1-1}+Q_{12}R^{m_2+n_1-1}+Q_{13}R^{n_1+n_2}\ln\left(R\right)+Q_{14}R^{n_1+n_2} \tag{55}$$

$$\bar{\sigma}_\theta=Q_{21}R^{m_1+n_1-1}+Q_{22}R^{m_2+n_1-1}+Q_{23}R^{n_1+n_2}\ln\left(R\right)+Q_{24}R^{n_1+n_2} \tag{56}$$

where:

$$\begin{aligned} Q_{11}&=\left(A_1m_1+A_2\right)C_1 & Q_{21}&=\left(A_2m_1+A_1\right)C_1 \\ Q_{12}&=\left(A_1m_2+A_2\right)C_2 & Q_{22}&=\left(A_2m_2+A_1\right)C_2 \\ Q_{13}&=\left(n_2+1\right)A_1C_3+A_2C_3-A_1D_1\Theta & Q_{23}&=\left(n_2+1\right)A_2C_3+A_1C_3-A_1D_1\Theta \\ Q_{14}&=A_1C_3+\left(n_2+1\right)A_1C_4+A_2C_4-A_1D_2\Theta & Q_{24}&=A_2C_3+\left(n_2+1\right)A_2C_4+A_1C_4-A_1D_2\Theta \end{aligned} \tag{57}$$

The constants C_1 and C_2, in this case, are gained by applying mechanical boundary conditions expressed in Eq. (45), i.e.

$$C_1=\left(-\frac{K^{n_1+n_3}\ln\left(K\right)}{K^{m_1+n_1-1}-K^{m_2+n_1-1}}Q_{13}+\frac{K^{m_2+n_1-1}-K^{n_1+n_3}}{K^{m_1+n_1-1}-K^{m_2+n_1-1}}Q_{14}+\frac{K^{m_2+n_1-1}-P^*}{K^{m_1+n_1-1}-K^{m_2+n_1-1}}\right)\Big/\left(A_1m_1+A_2\right) \tag{58}$$

$$C_2=\left(-\frac{K^{n_1+n_3}\ln\left(K\right)}{K^{m_2+n_1-1}-K^{m_1+n_1-1}}Q_{13}+\frac{K^{m_1+n_1-1}-K^{n_1+n_3}}{K^{m_2+n_1-1}-K^{m_1+n_1-1}}Q_{14}+\frac{K^{m_1+n_1-1}-P^*}{K^{m_2+n_1-1}-K^{m_1+n_1-1}}\right)\Big/\left(A_1m_2+A_2\right) \tag{59}$$

3.0 RESULTS AND DISCUSSIONS

In previous section, the governing equations of FGM thick-walled cylinder under mechanical and thermal loads were successfully derived using plane elasticity theory. In this section, a practical case study is investigated and the results are compared to that one obtained from elastic cylinders. Without any loss of generality, the inside and outside temperatures and relative pressures are assumed to be 25℃, 300℃, 80 MPa and zero, respectively. The elasticity modulus, Poisson's ratio, the coefficients of thermal expansion and heat conduction at the inner surface of the cylinder were selected as E_i = 200 GPa, v=0.3, α_i = 17.5×10^{-6} /◦C and k_i=15 W/mK, respectively. Due to use of R as dimensionless radius, the derived equations are independent on the inner (r_i) and outer (r_o) radii; however, the radii values of r_i=40 mm and r_o=60 mm were chosen to analyze the numerical solution. To better investigation, the results have been presented for various values of FGM parameter in the range of -2≤n≤2. In order to perform numerical analysis, a geometry sample was modeled using finite element method for a comparative study. The finite element (FE) model was constructed using COMSOL Multiphysics® software. The outputs of this simulation have been utilized to compare the thermo-elastic results obtained from both analytical and numerical solutions for the functionally graded thick-walled cylinder under a combination of mechanical and thermal loads.

Figure 2 shows the radial distribution of elasticity modulus E versus dimensionless radius R for various values of n. As can be observed from this figure, elasticity modulus is constant at inner surface for different values of n, while it increases at outer surface when n enhances from n=-2 to n=2. On the other hand, with attention.

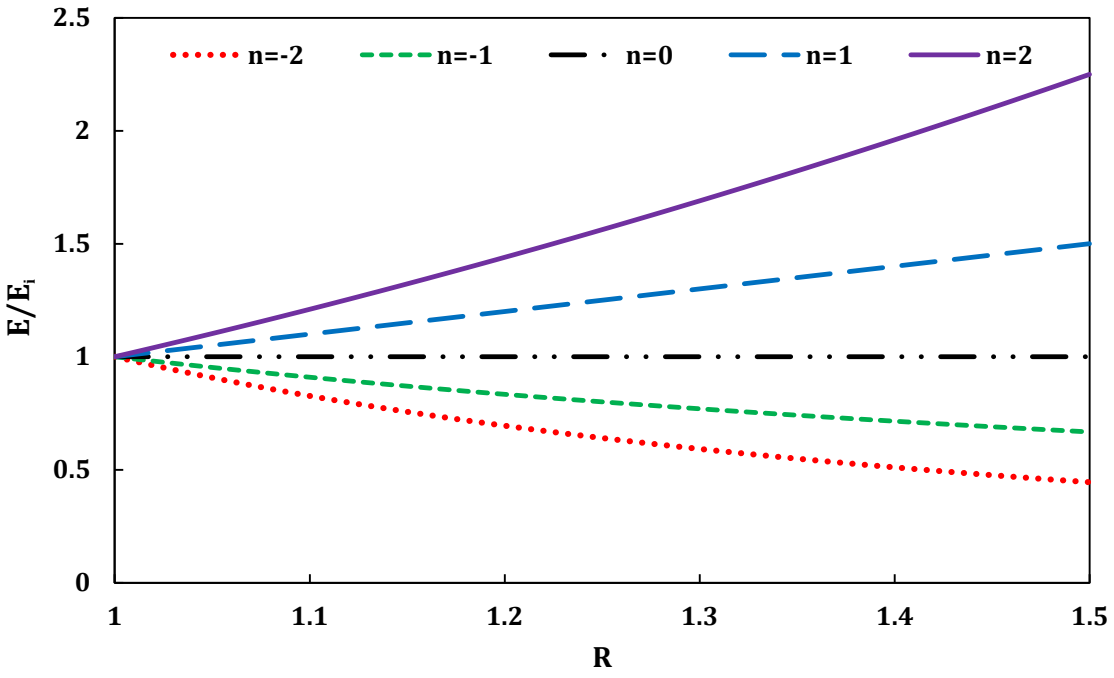

Figure 2. Radial distribution of elasticity modulus.

to the slope of elasticity modulus curves, it is seen that the absolute value of curve slopes for $n>0$, are greater than the case of $n<0$. Figure 3 indicates the radial distribution of temperature in homogeneous ($n=0$) and heterogeneous ($n\neq0$) cylinders in present work. As shown in this figure, the temperature reduces by increasing the value of n from $n=-2$ to $n=2$. Moreover, this figure reveals that the temperature decreases with an increase in radius.

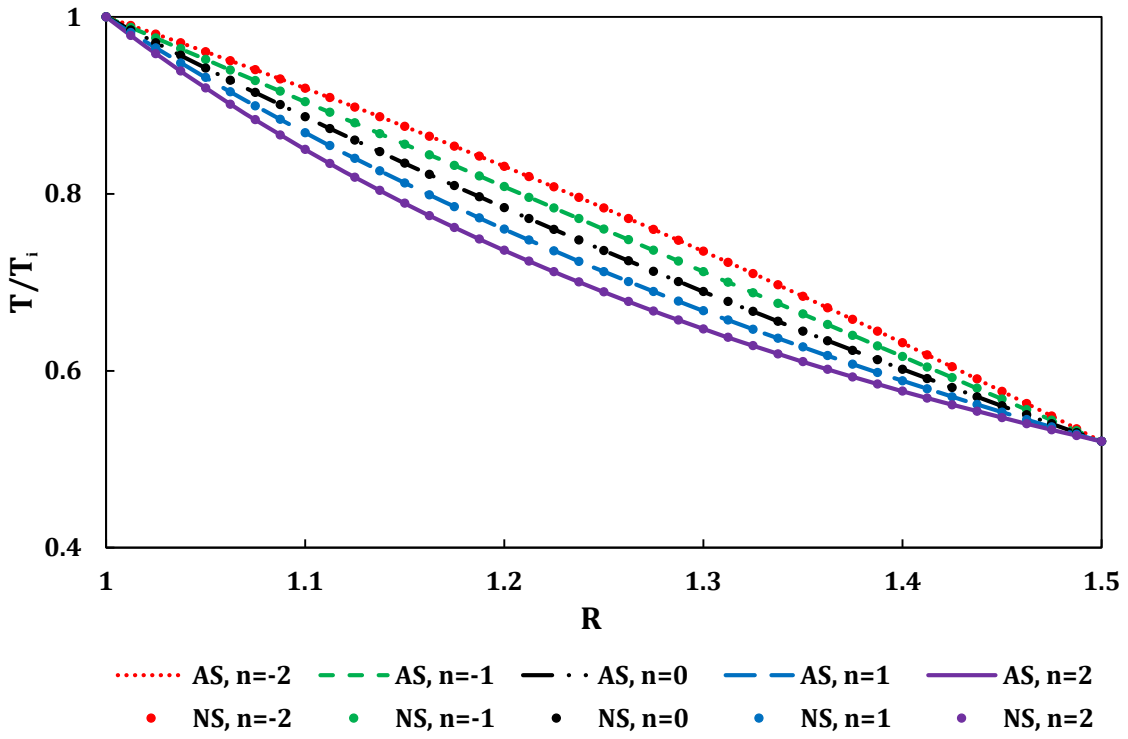

Figure 3. Distribution of the normalized radial temperature under the thermal loading.

Figure 4 demonstrates the dimensionless radial stress distribution $\bar{\sigma}_r$ versus dimensionless radius R in response of both analytical (AS) and numerical (NS) solutions. According to this figure, the magnitude of radial stress decreases/increases for $n<0$ / $n>0$, respectively. Therefore, this decrease and increase in the radial stress depends on $|n|$. Based on this figure, for non-dimensional radius $R<1.1$, the stress values for all amount of n are relatively close to each other; while, significant differences in stress values are seen for $R>1.1$.

The dimensionless circumferential stress $\bar{\sigma}_\theta$ versus dimensionless radius R for homogeneous ($n=0$) and heterogeneous ($n\neq0$) cylinders is plotted in Figure 5. According to this figure, circumferential stress for more negative values of n in internal, central and

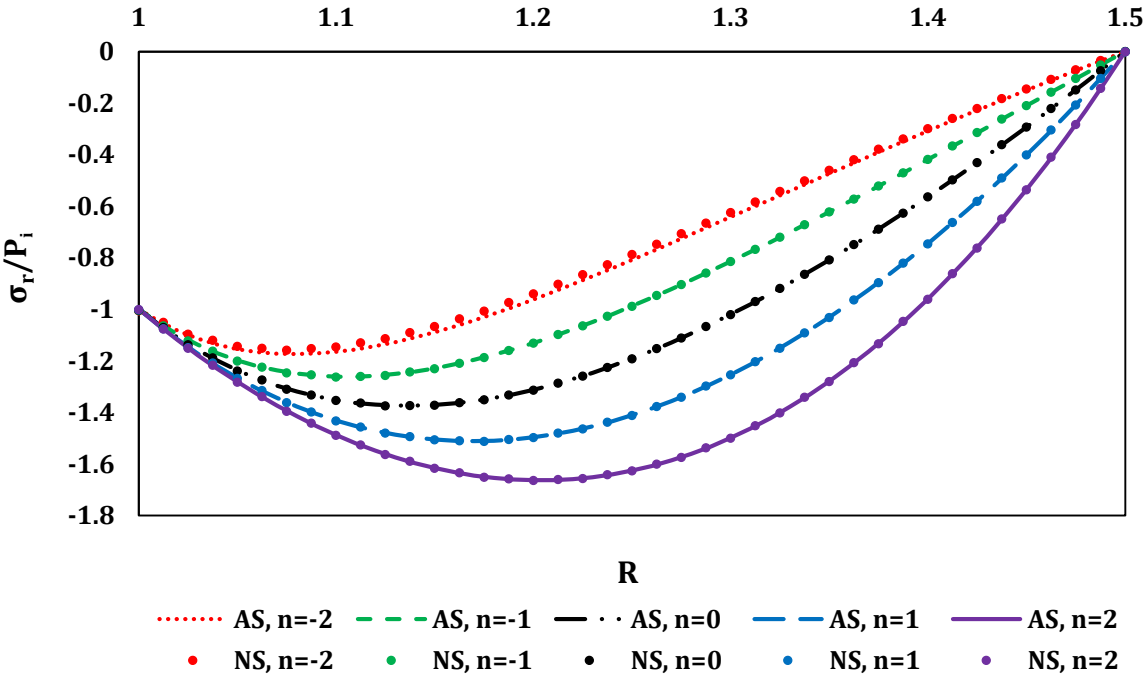

Figure 4. Normalized radial stress of homogeneous (n=0) and FGM heterogeneous (n≠0) cylinders under the combined thermo-mechanical loads.

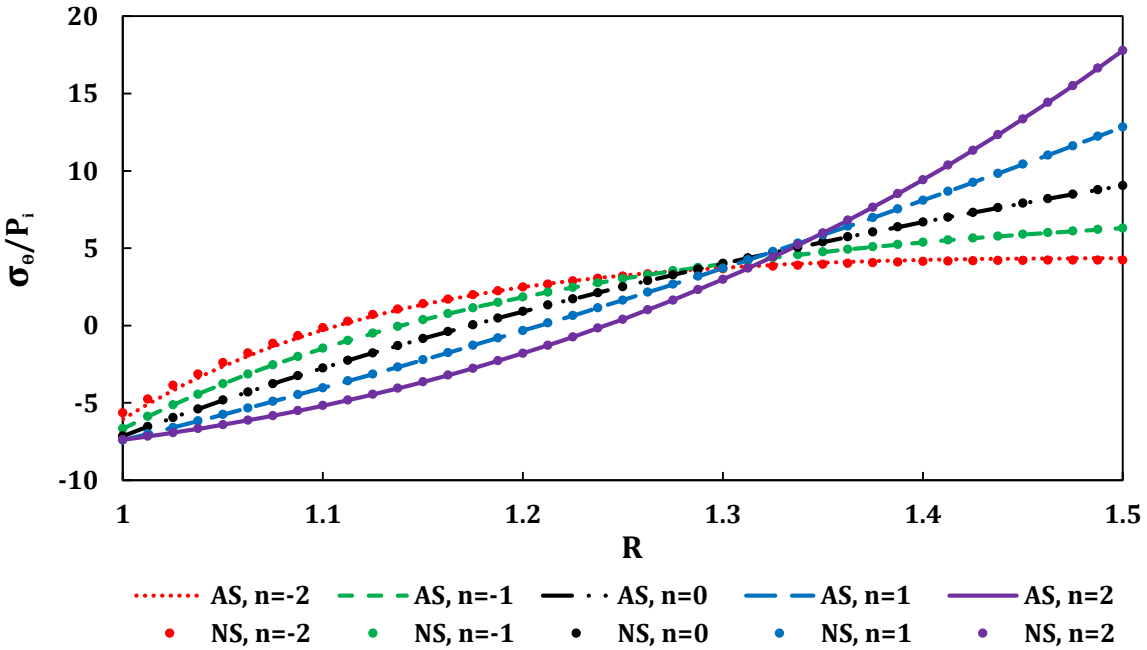

Figure 5. Normalized circumferential stress of homogeneous (n=0) and FGM heterogeneous (n≠0) cylinders under the combined thermo-mechanical loads.

external regions of cylinder is less than, equal to and higher than the corresponding homogeneous (n=0) cylinder respectively and vice versa for more positive values of n. In other words, with reference to this figure, it can be found that the curves of circumferential stress meet and cross each other in the range of $1.3 \leq R \leq 1.4$. Figures 4 and 5 can illustrate the important role of radial thickness in terms of radial and circumferential stresses in FGM thick-walled cylinder.

Figure 6 explains the distribution of normalized radial displacement versus non-dimensional radius R in homogeneous (n=0) and heterogeneous ($n \neq 0$) cylinders. As can be observed from this figure, the displacement of heterogeneous ($n \neq 0$) cylinder is lower than homogeneous (n=0) one for negative values of n and would be vice versa for $n>0$. This ratio, of course, is almost constant along the wall and the amount of differences depend on the magnitude of $|n|$.

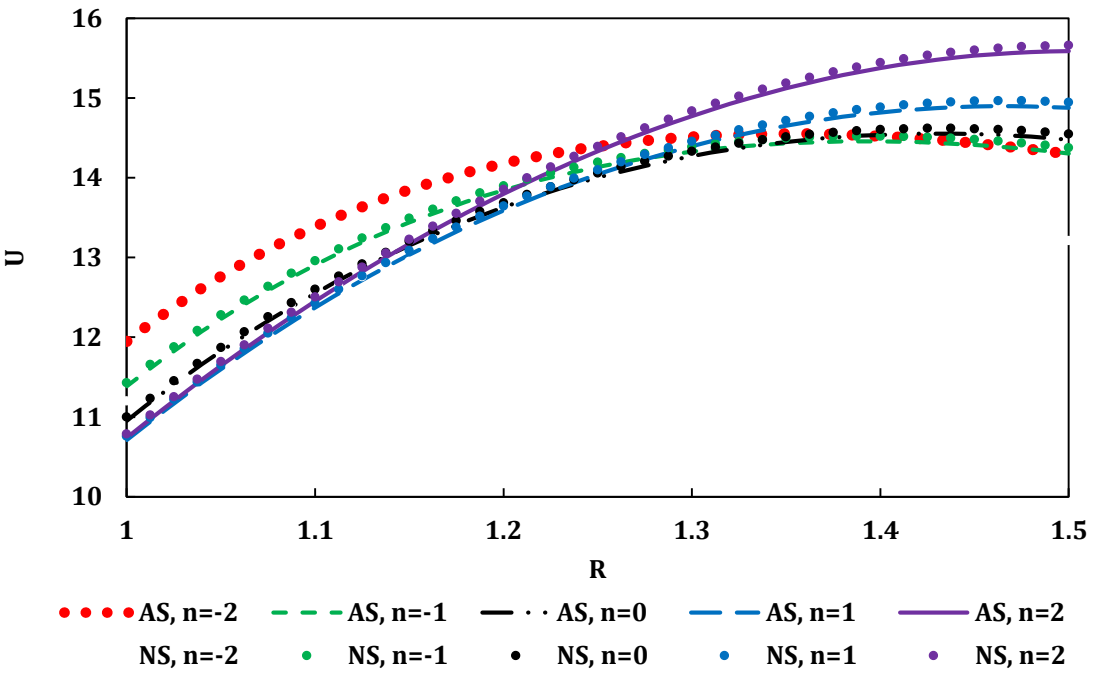

Figure 6. Normalized radial displacement of homogeneous (n=0) and FGM heterogeneous ($n \neq 0$) cylinders under the combined thermo-mechanical loads

Overall, according to the all above-mentioned results, it can be concluded that the radial and circumferential stresses and the radial displacement of FGM heterogeneous ($n \neq 0$) cylinder increase/decrease relative to the sign of n (positive or negative) so that whatever $|n|$ grows to be larger, more changes can be seen. Therefore, based on the need to decrease or increase in stress and displacement of FGM heterogeneous ($n \neq 0$), we can use the positive or negative n parameter in our design. Moreover, it can be found from Figures 4, 5 and 6 that there are good agreements between analytical (AS) and numerical (NS) solutions. These agreements give acceptable approvals on the governing equations obtained in this present study. The FEM contours of stresses and

displacements of both homogeneous (n=0) and FGM heterogeneous (n≠0) cylinders for all values of n are presented in Figure 7.

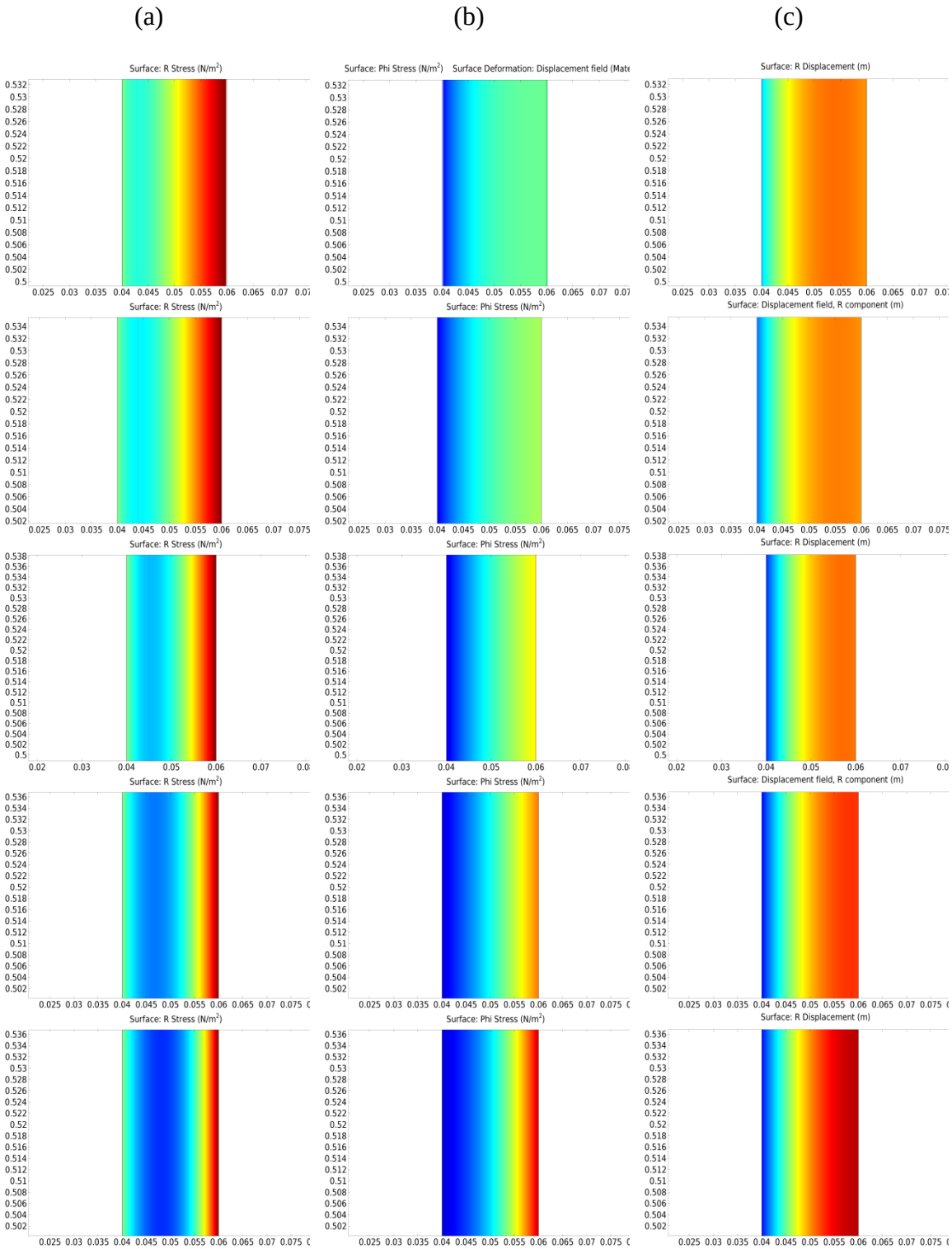

Figure 7. Distribution of (a) radial stress, (b) circumferential stress and (c) radial displacement of homogeneous (n=0) and FGM heterogeneous (n≠0) cylinders under the combined thermo-mechanical loads (Row No.1 to row No.5 are respectively related to: n=-2, -1, 0, 1, 2).

4.0 CONCLUSIONS

In this research, both the analytic and numeric solutions of homogeneous and FGM heterogeneous thick-walled cylinders were successfully performed under a combination of mechanical and thermal loads. The numerical results indicated that the governing equations, obtained in present work, are acceptable in order to analyze the homogeneous and FGM heterogeneous thick-walled cylinders under joint mechanical and thermal loads. They let somebody see and predict the optimum state of problem in terms of stress and displacement based on desired design requirements. It was found that the material parameter has great effects on the stress and displacement of FGM heterogeneous thick-walled cylinders. In other words, from a design point of view, they would be useful parameters as they can be tailored to specific applications in order to control the stress and displacement of thick-walled FGM cylinder.

REFERENCES

Argeso, H. A. & Eraslan, N. (2008). On the use of temperature-dependent physical properties in thermo mechanical calculations for solid and hollow cylinders, *International Journal of Thermal Sciences*, *47*, 136–146.

Azadi M., & Shariyat, M. (2010). Nonlinear transient transfinite element thermal analysis of thick-walled FGM cylinders with temperature-dependent material properties, *Meccanica*, *45*(3), 305-318.

Azadi, M. & Azadi M., (2009). Nonlinear transient heat transfer and thermoelastic analysis of thick-walled FGM cylinder with temperature-dependent material properties using Hermitian transfinite element, *Journal of Mechanical Science and Technology*, *23*(10), 2635-2644.

Bayat Y., Ghannad M., & H. Torabi. (2012). Analytical and numerical analysis for the FGM thick sphere under combined pressure and temperature loading, *Archive of Applied Mechanics*, *82*(2), 229-242.

Damircheli M., & Azadi M. (2011). Temperature and thickness effects on thermal and mechanical stresses of rotating FG-disks, *Journal of Mechanical Science and Technology*, *25*(3), 827-836.

Kreyszig E. (2010). *Advanced Engineering Mathematics*, John Wiley & Sons.

Mahamood R.M., Akinlabi T.A., Shukla M., & Pityana S. (2012). Functionally Graded Material: An Overview, *Proceedings of the World Congress on Engineering (WCE) 3*, 83-86.

Nejad M.Z., Abedi M., Lotfian M.H., & Ghannad M. (2012). An exact solution for stresses and displacements of pressurized FGM thick-walled spherical shells

with exponential-varying properties, *Journal of Mechanical Science and Technology*, *26*(12), 4081-4087.

Rohsenow, Warren M. (1998). *Handbook of Heat Transfer*. *Vol. 3*. New York: McGraw-Hill.

Tutuncu, N. & Ozturk, M. (2001). Exact solution for stresses in functionally graded pressure vessels, *Composites Part B: Engineering*, *32* (8), 683-686.